Graphene Q-switched 2.78 μm Er^{3+}-doped fluoride fiber laser

Chen Wei,[1] Xiushan Zhu,[1,3] F. Wang,[2,4] Y. Xu,[2] Kaushik Balakrishnan,[1] Feng Song,[1] Robert A. Norwood,[1] and N. Peyghambarian[1]

[1]*College of Optical Sciences, University of Arizona, 1630 E. University Blvd., Tucson, Arizona 85721, USA*

[2]*School of Electronic Science and Engineering, Nanjing University, Nanjing 210093, China*

[3]*e-mail: xszhu@email.arizona.edu*

[4]*e-mail: fwang@nju.edu.cn*

Received June 13, 2013; revised July 18, 2013; accepted July 21, 2013;
posted July 22, 2013 (Doc. ID 192233); published August 20, 2013

We report a diode-pumped 2.78 μm Er^{3+}-doped ZBLAN fiber laser passively Q switched by a graphene saturable absorber, which was directly deposited onto a fiber dichroic mirror by the method of optically driven deposition. Stable Q-switched operation with a pulse duration of 2.9 μs and a pulse energy of 1.67 μJ was achieved in a 10 m long gain fiber. The pulse duration was reduced to 1 μs when the gain fiber length was shortened to 2 m. This Letter demonstrates that graphene is a promising and reliable saturable absorber for mid-infrared pulse generation at 3 μm.

© 2013 Optical Society of America

OCIS codes: (140.3070) Infrared and far-infrared lasers; (140.3540) Lasers, Q-switched; (140.3500) Lasers, erbium; (140.3510) Lasers, fiber.

http://dx.doi.org/10.1364/OL.38.003233

Compact pulsed lasers operating in the 3 μm wavelength band have attracted much attention in recent years because of their many practical potential applications. 3 μm lasers (e.g., the Er^{3+}:YAG laser) have been used in vitreo-retinal surgery [1], dental tissue ablation [2], and cardiovascular surgery [3], due to the high absorption coefficient of water (in body tissues) at this wavelength [4,5]. Other potential applications of 3 μm lasers include spectroscopic sensors, optical pump sources for longer wavelength mid-infrared (mid-IR) or far-infrared oscillators, and infrared countermeasures. High-concentration Er^{3+}-doped ZBLAN fiber lasers [6], which emit mid-IR light in the 2.7–2.9 μm band through the ${}^4I_{11/2} \rightarrow {}^4I_{13/2}$ transition, have become one of the most promising candidates for these applications because of their superior properties including high efficiency and broad emission spectral range, and the ready availability of diode-pump lasers at the 975 and 795 nm absorption peaks of Er^{3+}. Several 10 W level continuous-wave (CW) Er^{3+}-doped ZBLAN fiber lasers at 3 μm have been demonstrated recently [6–8]. Pulsed operation of Er^{3+}-doped ZBLAN fiber lasers is also highly desired because of their much higher peak powers. Pulsed laser operation can generally be achieved by modulating the Q factor of the laser cavity with active/passive Q switching or mode-locking techniques. Various modulation devices, such as acousto-optic modulator/rotating mirrors [9,10], mechanical rotating shutters [11], semiconductor saturable absorbers [12,13], and transition metal-doped crystals [14,15], have been used to realize pulsed operation of fiber lasers at 3 μm. We have demonstrated Q-switched and mode-locked Er^{3+}-doped ZBLAN fiber lasers by using Fe^{2+}:ZnSe crystal as the saturable absorber. Q-switched pulses with pulse duration of 370 ns and peak power of 5.34 W were achieved at a repetition rate of 161 kHz [14]. CW mode-locked pulses with pulse duration of 19 ps and peak power of 50 W were obtained at a repetition rate of 55 MHz [15]. However, using bulk Fe^{2+}:ZnSe as the saturable absorber compromises the simplicity and compactness of the fiber laser cavity while also introducing stringent alignment requirements. Graphene, a two-dimensional (2D) atomic layer of carbon atoms, has emerged as an innovative and remarkable saturable absorber because of its low saturation intensity, ultrafast relaxation time, large modulation depth, and high damage threshold [16–18]. Most importantly, due to its zero energy band gap and linear energy dispersion relation, graphene exhibits a wide wavelength-independent saturable absorption, spanning visible to mid-IR wavelength bands [19]. Graphene Q-switched and mode-locked rare-earth-doped silica fiber lasers have been successfully demonstrated at a number of wavelengths within the 1–2 μm wavelength range [20–26]. Recently, a solid-state Cr:ZnSe laser operating at ~2.5 μm has been mode locked by a monolayer graphene saturable absorber [27]. These advances inspired us to investigate graphene as a saturable absorber for pulse generation in the 3 μm region. Graphene flakes with micrometer lateral size can be deposited on fiber end facets or made to surround side-polished or tapered fibers to give fiber-based saturable absorbers [28], which can be used to make compact Q-switched and mode-locked all-fiber lasers with high reliability. In this Letter, we report a Q-switched 2.78 μm Er^{3+}-doped ZBLAN fiber laser, in which a graphene-coated fiber mirror was used as the saturable absorber.

In our experiment, graphene dispersion was purchased from Graphene Supermarket, Inc. (concentration ~5 mg/L). The wavelength-independent absorption of graphene in the mid-IR range was confirmed by measuring the transmission of a silicon substrate with a few milliliters of graphene dispersion drop casted on the surface. Figure 1 shows the flat infrared transmission of graphene (the effect of substrate has been subtracted) in a wavelength range from 1.5 to 6.5 μm. The Raman spectroscopy of the graphene dispersion on quartz microscope slides was measured using a Horiba Jobin Yvon Raman system with a pump laser at 514 nm. The single

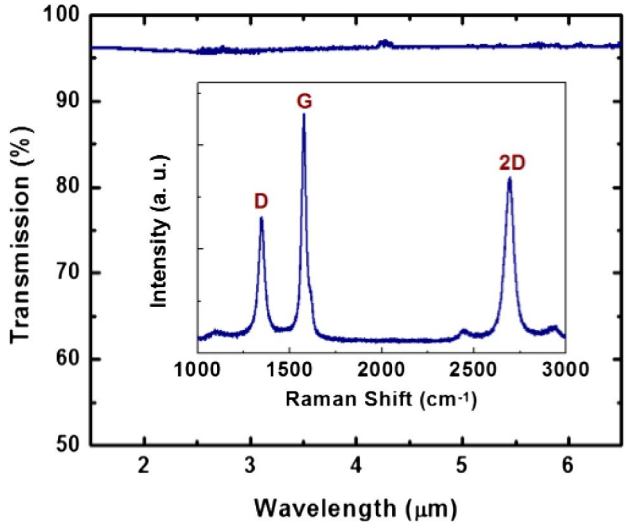

Fig. 1. Infrared transmission and Raman spectrum (inset) of graphene drop casted on silicon substrate.

Lorentzian shape of the 2D peak suggests the presence of a collection of electronically almost decoupled graphene monolayers. The relative large intensity of the D peak is contributed from the edge effects of small graphene flakes, rather than a high density of structural defects [18].

To make a fiber-based saturable absorber for the Er^{3+}-doped ZBLAN fiber laser, a fiber mirror was first fabricated by ion-beam deposition of a dichroic thin film (highly reflective at 2.8 μm and highly transparent at 976 nm) onto the end facet of a striped and cleaved optical fiber with a diameter of 125 μm. The fiber mirror was then spliced onto a fiber-coupled 976 nm diode laser and inserted into the graphene dispersion. Graphene flakes were deposited onto the end facet of fiber mirror by optical and thermal gradient forces [29]. We made use of optically driven deposition, with the power of the laser diode set to 25 mW and the deposition time at 5 min. The linear absorption of the deposited graphene was measured to be ~30% (−1.55 dB). The microscopic photographs of the fiber mirror before and after graphene deposition are shown in Figs. 2(a) and 2(b), respectively. Obviously, layers of graphene flakes were deposited onto the fiber mirror. It should be noted that, under our deposition conditions, the graphene flakes did not aggregate just at the core area, as observed in previous reports [29], but covered a much larger area on the end facet. We believe the thermal diffusion in the dielectric coating may have helped promote large area deposition of graphene

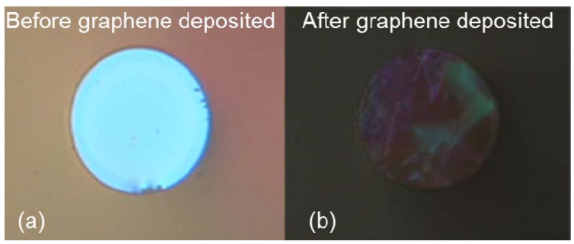

Fig. 2. Microscopic pictures of the fiber mirror end (a) before and (b) after graphene deposition.

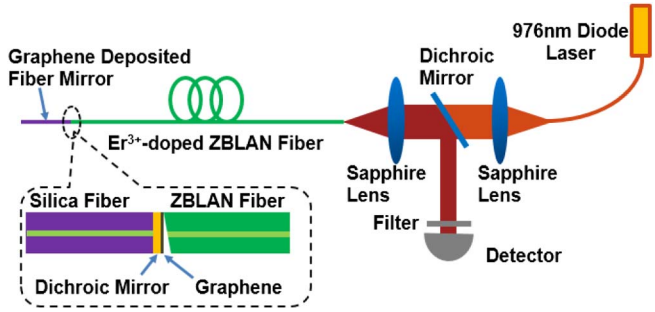

Fig. 3. Schematic setup of the graphene passively Q-switched Er^{3+}-doped ZBLAN fiber laser.

flakes. Further investigation and interpretation of this exciting phenomenon are currently underway.

The graphene passively Q-switched Er^{3+}-doped ZBLAN fiber laser was constructed in a linear cavity, as shown in Fig. 3. A 10 m high-concentration (8 mol. %) Er^{3+}-doped double-cladding ZBLAN fiber was used as the gain medium. The core of the gain fiber has a diameter of 15 μm and a numerical aperture of 0.1. The normalized frequency (V number) of this fiber is 1.7 for the 2.8 μm light, guaranteeing a single-transverse mode output laser beam with excellent beam quality. The inner cladding of the fiber has a diameter of 125 μm and a NA of 0.4. The gain fiber was cladding pumped by a 976 nm multimode laser diode. The pump absorption of the gain fiber was measured to be 6.5 dB/m by a cutback experiment. The pump laser was first collimated and then focused into the fiber inner cladding by two identical antireflection-coated plano-convex sapphire lenses with focal lengths of 25 mm. The flat cleaved end of the Er^{3+}-doped ZBLAN fiber was used as the output coupler mirror with ~4% Fresnel reflection. The other end of the gain fiber was angle cleaved (~8°) to eliminate the influence of the Fresnel reflection. The graphene deposited fiber dichroic mirror was directly butted against the angle cleaved fiber end as shown in the inset of Fig. 3. The output laser beam was coupled out with a dichroic mirror inserted between the two sapphire lenses at 45° to the collimated pumping beam. The background light was removed by a long-pass filter (>2 μm) placed in front of the detector.

The fiber laser started to Q switch at a pump power of 207.2 mW. However, the pulse trains were unstable. Stable, passively Q-switched pulses occurred at a pump power of 406.4 mW, with a repetition rate of 18.9 kHz and pulse energy of 0.74 μJ. The pulse trains were detected with a fast InSb infrared detector (rise time 7 ns) and recorded with an oscilloscope with 100 MHz bandwidth. The typical oscilloscope traces of the Q-switched pulse trains are shown in Fig. 4(a). As we increased the pump power from 406.4 to 828 mW, the pulse repetition rate of the Q-switched Er^{3+}-doped ZBLAN fiber laser changed from 18.9 to 37.2 kHz. The Q-switched pulse output was stable, and no significant pulse jitter was observed in this pump power region. Figure 4(b) shows the stable pulse trains under the maximum pump power of 828 mW. The pulse envelop of the Q-switched pulses at 828 mW pump power is shown in Fig. 4(c) (blue curve), which shows that a pulse duration of 2.9 μs was obtained in the 10 m Er^{3+}-doped ZBLAN fiber laser. The

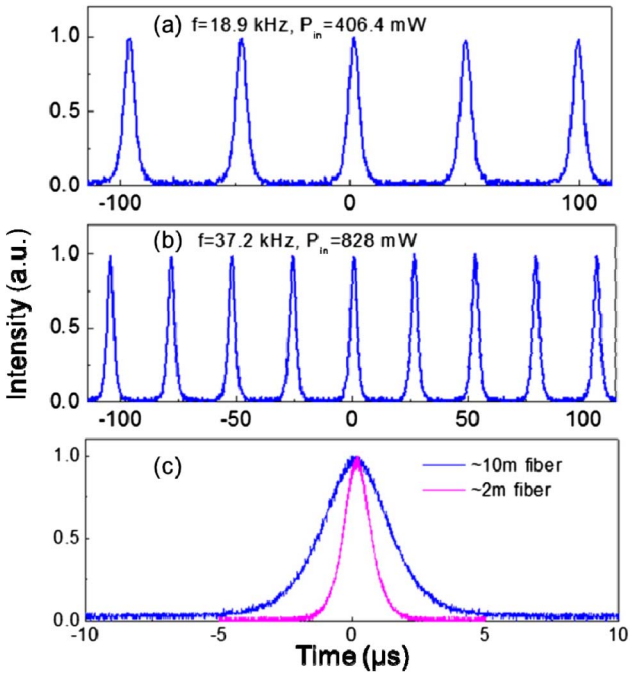

Fig. 4. Typical Q-switched pulse trains at pump powers of (a) 406.4 mW and (b) 828 mW; (c) pulse envelopes of the shortest stable pulses obtained in 10 m (blue curve) and 2 m (magenta curve) gain fibers.

radio-frequency (RF) spectrum of the fiber laser pumped at 406 mW was measured and is shown in Fig. 5. The signal-to-noise ratio was larger than 30 dB, indicating a fairly stable Q-switched operation. When the pump power was further increased, the Q-switched operation of the Er^{3+}-doped ZBLAN fiber laser was not stable, with noticeable amplitude fluctuation and timing jitter, which may have been caused by thermal effects in the graphene absorber. The pulsed operation was extinguished eventually at 930 mW due to catastrophic damage to the graphene film. The spectrum of the Q-switched Er^{3+}-doped ZBLAN fiber laser was measured with a monochromator (SPEX 270) with a resolution of 1 nm and is shown in Fig. 6. The 3 dB bandwidth is ~2 nm, and the center wavelength is about 2783 nm, which is a typical lasing wavelength for a high-concentration Er^{3+}-doped ZBLAN fiber laser.

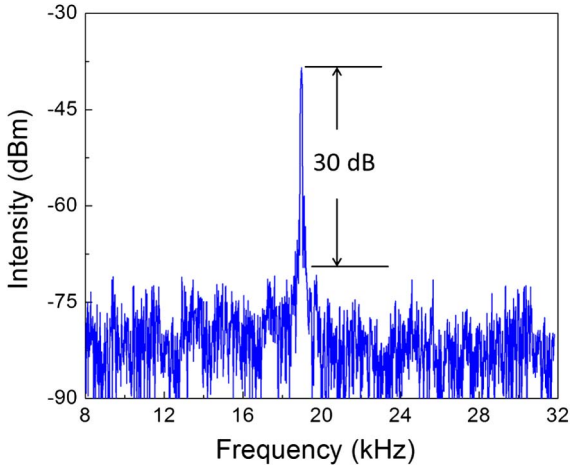

Fig. 5. RF spectrum of the graphene passively Q-switched Er^{3+}-doped ZBLAN fiber laser pumped at 406 mW.

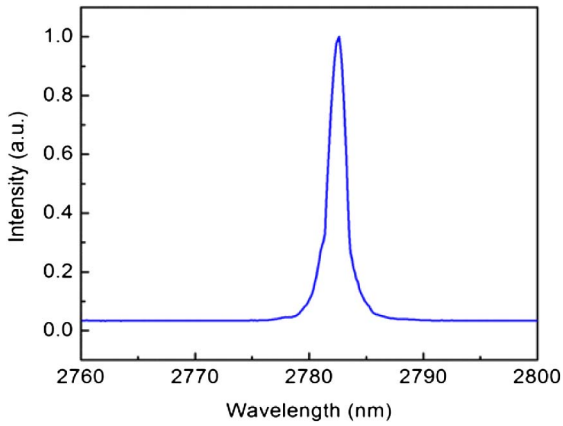

Fig. 6. Spectrum of the Er^{3+}-doped ZBLAN fiber laser Q-switched by the graphene thin film.

The pulse duration and pulse repetition rate as a function of the pump power were measured and are shown in Fig. 7. As observed in typical Q-switched fiber lasers, the pulse duration decreases while the repetition rate increases almost linearly with increased pump power in the stable Q-switched operation regime. Figure 8 shows the average output power measured with a thermal power meter and the calculated pulse energy as a function of the pump power. The pulse energy and average output power of the stable Q-switched fiber laser both increased monotonically with the increased pump power. At a pump power of 828 mW, a maximum pulse energy of 1.67 μJ with a repetition rate of 37 kHz, and a maximum average output power of 62 mW, were achieved. The slope efficiency of the 10 m long Q-switched Er^{3+}-doped ZBLAN fiber laser was 10.5%.

According to previous experimental results on graphene Q-switched silica fiber lasers, shorter pulses can generally be obtained in a shorter fiber cavity [20]. In order to obtain shorter pulses, we used a 2 m Er^{3+}-doped ZBLAN fiber without changing other components in the fiber cavity, and a minimum pulse duration of 1 μs was achieved [shown by the magenta curve in Fig. 4(c)]. The threshold of the Q-switched operation was ~420 mW, and the maximum output average power was ~65 mW.

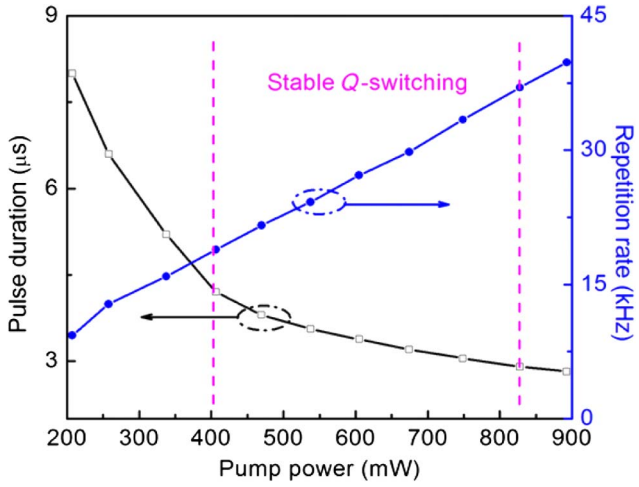

Fig. 7. Pulse duration (black line with squares) and repetition rate (blue line with circles) as a function of the pump power.

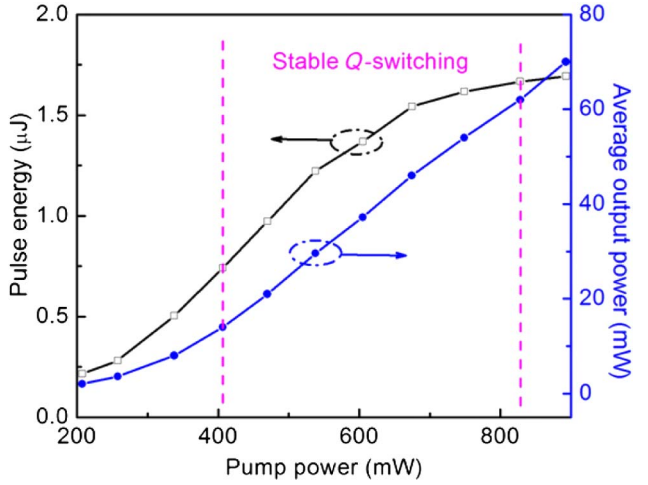

Fig. 8. Pulse energy (black line with squares) and average output power (blue line with circles) as a function of the pump power.

The slope efficiency of the 2 m long Q-switched Er^{3+}-doped ZBLAN fiber laser was ~8.8%. Q-switched operation of the 2 m fiber laser, however, was not as stable as for the 10 m one. This is probably due to the large thermal effect of the graphene saturable absorber caused by the residual pump power. It is expected that stable nanosecond pulses can be obtained by employing a shorter fiber cavity as well as reducing the residual pump power launched at the graphene thin film.

In conclusion, a compact, graphene Q-switched Er^{3+}-doped ZBLAN fiber laser at 2.78 μm was demonstrated. Stable Q-switched pulses with a pulse duration of 2.9 μs and a pulse energy of up to 1.67 μJ at a repetition rate of 37 kHz have been obtained. Mode-locked operation of this fiber laser has not been observed in our experiment. This may derive from the unoptimized parameter range of the graphene saturable absorber and/or the current laser cavity design. Further investigation into mode-locked operation of Er^{3+}-doped ZBLAN fiber lasers by optimizing the graphene linear and nonlinear absorption and increasing the Q factor of the fiber cavity is currently underway.

This work was supported by the National Science Foundation Engineering Research Center for Integrated Access Networks (grant no. EEC-0812072) and the Photonics Initiative of the University of Arizona (TRIF). The authors thank Dmitry Churin for help in the optical spectrum measurement.

References

1. Q. Ren, V. Venugopalan, K. Schomacker, T. F. Deutsch, T. J. Flotte, C. A. Puliafito, and R. Birngruber, Lasers Surg. Med. **12**, 274 (1992).
2. H. A. Wigdor, J. T. Walsh, Jr., J. D. Featherstone, S. R. Visuri, D. Fried, and J. L. Waldvogel, Lasers Surg. Med. **16**, 103 (1995).
3. L. I. Deckelbaum, Lasers Surg. Med. **15**, 315 (1994).
4. J. Kampmeier, S. Schafer, G. E. Lang, and G. K. Lang, J. Refract. Surg. **15**, 563 (1999).
5. P. Werle, F. Slemr, K. Maurer, R. Kormann, R. Mucke, and B. Janker, Opt. Lasers Eng. **37**, 101 (2002).
6. X. Zhu and R. Jain, Opt. Lett. **32**, 26 (2007).
7. S. Tokita, M. Murakami, S. Shimizu, M. Hashida, and S. Sakabe, Opt. Lett. **34**, 3062 (2009).
8. D. Faucher, M. Bernier, G. Androz, N. Caron, and R. Vallée, Opt. Lett. **36**, 1104 (2011).
9. C. Frerichs and T. Tauermann, Electron. Lett. **30**, 706 (1994).
10. T. Shigeki, M. Masanao, S. Seiji, H. Masaki, and S. Shuji, Opt. Lett. **36**, 2812 (2011).
11. D. J. Coleman, T. A. King, D. K. Ko, and J. Lee, Opt. Commun. **236**, 379 (2004).
12. C. Frerichs and U. B. Unrau, Opt. Fiber Technol. **2**, 358 (1996).
13. J. Li, D. D. Hudson, Y. Liu, and S. D. Jackson, Opt. Lett. **37**, 3747 (2012).
14. C. Wei, X. Zhu, R. A. Norwood, and N. Peyghambarian, IEEE Photon. Technol. Lett. **24**, 1741 (2012).
15. C. Wei, X. Zhu, R. Norwood, and N. Peyghambarian, Opt. Lett. **37**, 3849 (2012).
16. A. K. Geim and K. S. Novoselov, Nat. Mater. **6**, 183 (2007).
17. Q. L. Bao, H. Zhang, Y. Wang, Z. Ni, Y. Yan, Z. X. Shen, K. P. Loh, and D. Y. Tang, Adv. Funct. Mater. **19**, 3077 (2009).
18. Z. Sun, T. Hasan, F. Torrisi, D. Popa, G. Privitera, F. Wang, F. Bonaccorso, D. M. Basko, and A. C. Ferrari, ACS Nano **4**, 803 (2010).
19. J. M. Dawlaty, S. Shivaraman, J. Strait, P. George, M. Chandrashekhar, F. Rana, M. G. Spencer, D. Veksler, and Y. Chen, Appl. Phys. Lett. **93**, 131905 (2008).
20. J. Liu, S. Wu, Q. Yang, and P. Wang, Opt. Lett. **36**, 4008 (2011).
21. H. Zhang, Q. L. Bao, D. Y. Tang, L. M. Zhao, and K. P. Loh, Appl. Phys. Lett. **95**, 141103 (2009).
22. Y. W. Song, S. Y. Jang, W. S. Han, and M. K. Bae, Appl. Phys. Lett. **96**, 051122 (2010).
23. H. Zhang, D. Y. Tang, L. M. Zhao, Q. L. Bao, and K. P. Loh, Opt. Express **17**, 17630 (2009).
24. J. Liu, J. Xu, and P. Wang, Opt. Commun. **285**, 5319 (2012).
25. F. Wang, F. Torrisi, Z. Jiang, D. Popa, T. Hasan, Z. Sun, W. Cho, and A. C. Ferrari, in *Proceedings of Conference on Lasers and Electro-Optics* (2012), paper JW2A.72.
26. M. Zhang, E. J. R. Kelleher, F. Torrisi, Z. Sun, T. Hasan, D. Popa, F. Wang, A. C. Ferrari, S. V. Popov, and J. R. Taylor, Opt. Express **20**, 25077 (2012).
27. M. N. Cizmeciyan, J. W. Kim, S. Bae, B. H. Hong, F. Rotermund, and A. Sennaroglu, Opt. Lett. **38**, 341 (2013).
28. S. Yamashita, J. Lightwave Technol. **30**, 427 (2012).
29. J. W. Nicholson, R. S. Windeler, and D. J. di Giovanni, Opt. Express **15**, 9176 (2007).